2021 43rd Annual International Conference of the
IEEE Engineering in Medicine & Biology Society (EMBC)
Oct 31 - Nov 4, 2021. Virtual Conference

High-Resolution Label-Free Molecular Imaging of Brain Tumor

Rong Guo, *Student Member, IEEE*, Chao Ma, Yudu Li, *Student Member, IEEE*, Yibo Zhao, Tianyao Wang, Yao Li, Georges El Fakhri and Zhi-Pei Liang, *Fellow, IEEE*

Abstract — **Molecular imaging has long been recognized as an important tool for diagnosis, characterization, and monitoring of treatment responses of brain tumors. Magnetic resonance spectroscopic imaging (MRSI) is a label-free molecular imaging technique capable of mapping metabolite distributions non-invasively. Several metabolites detectable by MRSI, including Choline, Lactate and N-Acetyl Aspartate, have been proved useful biomarkers for brain tumor characterization. However, clinical application of MRSI has been limited by poor resolution, small spatial coverage, low signal-to-noise ratio and long scan time. This work presents a novel MRSI method for fast, high-resolution metabolic imaging of brain tumor. This method synergistically integrates fast acquisition sequence, sparse sampling, subspace modeling and machine learning to enable 3D mapping of brain metabolites with a spatial resolution of 2.0×3.0×3.0 mm^3 in a 7-minute scan. Experimental results obtained from patients with diagnosed brain tumor showed great promise for capturing small-size tumors and revealing intra-tumor metabolic heterogeneities.**

Clinical Relevance — **This paper presents a novel technique for label-free molecular imaging of brain tumor. With further development, this technology may enable many potential clinical applications, from tumor detection, characterization, to assessment of treatment efficacy.**

I. Introduction

Noninvasive molecular imaging of brain tumor has been a dream of imaging scientists and clinicians [1]–[3]. Knowledge of tissue metabolism is essential for diagnosis, treatment planning and therapeutic assessment of brain tumor [2]–[7]. Magnetic resonance imaging (MRI) techniques have been widely used in clinical practice to provide structural information, which is sensitive to neoplastic diseases but not specific for the definition of the borders of tumoral involvement. There are several important clinical questions that cannot be elucidated by structural imaging alone but potentially with the help of metabolic imaging, including: differentiating tumors with other focal lesions, differentiating tumors of different grades and mutant phenotypes, evaluating metabolic heterogeneities of tumor, delineating tumor boundaries, and monitoring responses to treatment [7], [8].

Molecular imaging techniques like positron emission tomography (PET) have been used for imaging brain tumor metabolism although their clinical use has been limited by the accessibility to specific radioactive tracers [9], [10]. Magnetic resonance spectroscopic imaging (MRSI) is a label-free molecular imaging technique that has long shown great promise in capturing metabolic abnormality in brain tumors [2], [7]. Numerous studies in the past several decades have shown the clinical values of brain metabolites including N-Acetyl Aspartate (NAA), Choline (Cho), Creatine (Cr) and Lactate (Lac) as biomarkers for differentiation between high-grade and low-grade tumors, and between neoplastic and non-neoplastic lesions. Spectra of brain tumors typically show decreased NAA (related to neuron loss) and increased Cho (associated with tumor cell proliferation) compared to normal brain tissue. [2]–[7].

However, due to the low concentration of brain metabolites (<1,000th of water) and the requirement of large number of measured data samples, conventional MRSI techniques take long scan time (~20 minutes) and are limited to single voxel measurements or single slice imaging with low-resolution (~1 cm^3) [2], [7]. The limited spatial coverage and low resolution of conventional MRSI techniques make it difficult to capture whole-brain metabolic changes and metabolic alterations of small tumors, which have been a major obstacle for widespread clinical use. To overcome these difficulties, dedicated efforts have been made in the past decades to improve the imaging capability of MRSI, including special excitation pulses [11], [12], fast sampling trajectories [13]–[15] and advanced processing methods [16]–[18]. However, MRSI has yet been widely accepted as a routine clinical tool due to inadequate spatial resolution and imaging speed.

In this paper, we present a novel MRSI method for fast, high-resolution mapping of brain tumor metabolism. This method utilizes the subspace imaging framework in SPICE (Spectroscopic Imaging by exploiting spatiospectral CorrElation) [19]–[27] to synergistically integrate fast scanning, sparse sampling, subspace modeling and machine learning strategies. The proposed method has enabled volumetric mapping of brain metabolites with a spatial resolution of 2.0×3.0×3.0 mm^3 in a 7-minute scan. Experimental results demonstrated an impressive imaging capability to map the metabolic heterogeneities of tumor and delineate small-size tumors.

The rest of the paper is organized as follows: Section II describes the method in detail including data acquisition and image reconstruction, Section III shows representative in vivo results obtained from tumor patients, and Section IV concludes the paper.

*Corresponding author: Rong Guo; phone: 217-693-9862; e-mail: rongguo2@illinois.edu.

R. Guo, Y. Zhao, Y. Li, and Z.-P. Liang are with the Department of Electrical and Computer Engineering and Beckman Institute for Advanced Science and Technology, University of Illinois at Urbana-Champaign, Urbana, IL 61801 USA.

C. Ma and G. El Fakhri are with Gordon Center for Medical Imaging, Massachusetts General Hospital, Harvard Medical School, Boston, MA 02114, USA

T. Wang is with the Radiology Department, Shanghai Fifth People's Hospital, Fudan University, Shanghai, China.

Y. Li is with the School of Biomedical Engineering, Shanghai Jiao Tong University, Shanghai, China.

II. Proposed Method

The proposed method includes a special data acquisition scheme for fast imaging and a novel model-based method for image reconstruction. For fast high-resolution data acquisition, a special sequence was developed to achieve rapid scanning and sparse sampling of (k, t)-space; for image reconstruction, a union-of-subspaces model and subspace learning strategies were developed for effective nuisance signal removal and high-quality reconstruction from highly-undersampled, noise-corrupted (k, t)-space data.

A. Data acquisition

The proposed pulse sequence is illustrated in Fig. 1. To enable rapid scanning, the proposed pulse sequence used a short TR of 160 ms which is about a factor of 10 shorter than the TR used in traditional MRSI methods. This short TR was achieved by employing FID (free induction decay)-based acquisition with ultrashort TE (instead of spin echo-based acquisition with long TE) and eliminating the traditional lengthy pulses for water and lipid suppression. The removal of water suppression pulses also enabled simultaneous collection of unsuppressed water signals, which were utilized for correcting system imperfections (e.g., field inhomogeneity and field drift). To achieve high-resolution MRSI, rapid EPSI (echo planar spectroscopic imaging) trajectories with a large echo-space (1.76 ms) were used to obtain a resolution of 2 mm in the readout direction. As shown in Fig. 1(B), the EPSI trajectories enabled large coverage of k-space at the expense of reducing spectral encodings, which was handled by our processing method. Moreover, to increase the resolution in the phase encoding directions within a short scan time, the (k, t)-space was sparsely sampled with variable density (shown in Fig. 1(C)). More specifically, central k-space region was fully sampled for metabolic imaging while peripheral (k, t)-space was sparsely sampled by a factor of 36 below the Nyquist sampling density using CAIPIRINHA (controlled aliasing in parallel imaging results in higher acceleration) trajectories so as to achieve high resolution for the water signals [25]. Combining these unique features, the proposed pulse sequence was able to acquire 3D metabolite signals at 2.0×3.0×3.0 mm^3 resolution and water signals at 2.0×1.0×1.0 mm^3 resolution in a 7-minute scan.

B. Image reconstruction

With our data acquisition scheme, spectroscopic signals from different molecules (i.e., water, lipids, and metabolites) were simultaneously acquired in sparse measurements. The key processing issue lies in the separation and reconstruction of the spatiospectral functions from different molecules. We successfully solved this problem using a union-of-subspaces model-based method [25]. In our model, the spatiospectral function of each molecule ($\rho_n(x,t)$) was assumed residing in a very low-dimensional subspace, and the overall signal ($\rho(x,t)$) in the union of these subspaces:

$$\rho(x,t) = \sum_{n=1}^{N}\rho_n(x,t) = \sum_{n=1}^{N}\sum_{l=1}^{L_n} u_{n,l}(x)\, v_{n,l}(t), \quad (1)$$

where $v_{n,l}(t)$ denotes the temporal basis function for the n^{th} molecule (including water and lipids) and $u_{n,l}(x)$ the corresponding spatial coefficients. In practice, the model order L_n is much lower than the number of encodings, thus this subspace model significantly reduces the degrees-of-freedom

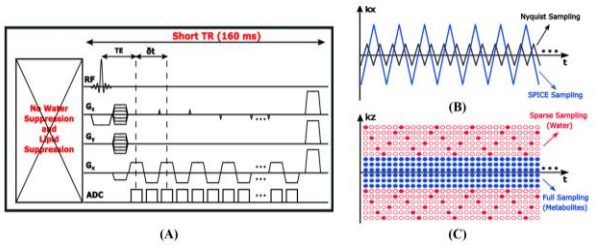

Figure 1. The proposed data acquisition scheme. (A) Pulse sequence diagram: no water/lipid suppression pulses were applied; FID signals were acquired in EPSI trajectories with ultra-short TE (1.6 ms) and short TR (160 ms); blip phase gradients were used to extend k-space coverage. (B) (kx, t)-space EPSI trajectories with large echospace (1.76 ms) to achieve high resolution in the readout direction. (C) (kz, t)-space CAIPIRINHA trajectories for sparse sampling (acceleration factor: 36) to achieve high-resolution in the phase encoding directions, with central k-space being fully sampled for metabolite signals.

[19]. This union-of-subspaces model not only facilitates reconstruction from sparse data and separation between different molecules, but also enables effective incorporation of spectral and spatial priors [22], [25].

In this work, the temporal basis functions of different molecules were pre-determined through subspace learning strategies, which provided very strong spectral priors [26]. More specifically, the subspaces of water and lipid signals (which have adequate SNR) were estimated from a set of high-resolution non-water-suppressed MRSI training data; the subspaces of low-concentration molecules were estimated from a set of high-SNR, relatively low-resolution water-suppressed MRSI training data. To capture the spectral distributions of molecules in both healthy and tumoral tissues, the training data were acquired from both healthy subjects and patients with diagnosed brain tumors.

With the learned signal subspaces capturing distinct spectral characteristics of different molecules, their spatiospectral functions can be separated and reconstructed effectively. Considering the significant concentration differences between nuisance and metabolite signals, we used a two-step strategy to reconstruct water/lipid and metabolite signals separately. We first solved the following optimization problem to reconstruct the water and lipid signals from the sparse data:

$$\hat{U}_w, \hat{U}_f = \arg\min_{U_w,U_f} \sum_{c=1}^{C}\left\| d_c - \Omega\{\mathcal{F}S_c \odot B \odot (M_w U_w V_w + M_f U_f V_f)\}\right\|_2^2 + \lambda_w \|DU_w\|_2^2 + \lambda_f \|DU_f\|_2^2, \quad (2)$$

where d_c is the vector form of the measured data from c^{th} coil, V_w, V_f are the matrix representations of the basis functions of water and lipid, respectively and U_w, U_f are the corresponding spatial coefficients. M_w, M_f are the spatial supports of brain tissue and subcutaneous lipids. Ω, $\mathcal{F}$, S_c, B, and D are the operators representing k-space sampling, Fourier transform, sensitivity encoding, field inhomogeneity, and edge-preserved total variation, respectively. The regularization parameters λ_w and λ_f were chosen based on the discrepancy principle. Once $\hat{U}_w$ and $\hat{U}_f$ determined, the spatiospectral functions of water and lipid can be synthesized as $\rho_w = \hat{U}_w V_w$ and $\rho_f = \hat{U}_f V_f$. Water and lipid signals were then removed from the measured central k-space, resulting in the noisy measurements of low concentration molecules. We solved the following optimization problem to reconstruct the spatiospectral function of these molecules using the learned subspaces:

$$\hat{U}_m = \arg\min_{U_m} \left\| d_r - \mathcal{F}\left(\sum_{m=1}^{M} U_m V_m\right) \right\|_2^2 + \sum_{m=1}^{M} \lambda_m \| D U_m \|_2^2, \quad (3)$$

where d_r is the vector form of the water/lipid removed (k, t)-space data after field correction and coil combination, V_m represent the pre-learned basis functions of the m^{th} molecule and U_m are the corresponding spatial coefficients to be determined. The second term of the cost function were spatial constraints imposed to further improve the SNR. The spatiospectral functions of different molecules can be generated as $\rho_m = U_m V_m$. Finally, the concentrations of different molecules can be estimated from the spatiospectral functions via spectral quantification [23].

C. In vivo experiment

All scans were performed on a 3T Skyra MR scanner (Siemens Healthineers, Erlangen, Germany) approved by the Institutional Review Board of Shanghai Fifth People's Hospital, China. Sixteen patients with diagnosed brain tumor were recruited (9 females, 7 males). Written informed consents were obtained from all participants. The imaging protocols include contrast enhanced MRPAGE (1.0×1.0×1.0 mm^3), T2 weighted FLAIR (0.5×0.5×2.0 mm^3), and ^{1}H-MRSI using SPICE (2.0×3.0×3.0 mm^3 for metabolite signals and 2.0×1.0×1.0 mm^3 for water signals, FOV= 240×240×72 mm^3, TR = 160 ms, TE = 1.6 ms, 7 minutes). The same SPICE sequence was used to acquire high-resolution training data for the water and lipid signals. A semi-LASER CSI sequence (10×10×10 mm^3, FOV = 240×240 mm^2, TR = 1200 ms, TE = 40 ms) was used to acquire training data for metabolite signals.

III. Results

Fig. 2 shows a representative set of high-resolution MRSI results (2.0×3.0×3.0 mm^3) obtained from a patient, comparing with the low-resolution counterpart with a practically used resolution (12×12×12 mm^3). The small tumor as indicated by the blue arrow in the anatomical image can be clearly observed on the high-resolution Cho map but is not differentiable from surrounding tissues in the low-resolution map. The spatially localized spectra also showed reduced NAA and elevated Cho in the tumor compared with the normal tissues, which is consistent with previous studies [2], [7]. In the low-resolution data, due to the significant partial volume effects, the spectral features were not as distinguishable from the normal issues as in the high-resolution MRSI data.

High-grade brain tumors like glioblastomas usually come with strong intra-tumoral heterogeneities; different regions such as edema, enhancing ring and necrotic core have different pathological conditions thus different metabolic fingerprints. As depicted in Fig. 3, four representative localized spectra from enhancing ring, surrounding edema, necrotic core and normal tissue showed distinct metabolic features. Edema, enhancing ring and edema all showed reduction of NAA due to the loss of neurons; enhancing ring where has the highest possibility of proliferation showed the highest Cho while necrotic cores showed reduction of all the metabolites. These metabolic heterogeneities can be clearly observed spatially on the metabolite maps in high-resolution.

Comparison of MRSI results obtained from low-grade tumor (WHO grade I) and high-grade tumor (WHO grade IV) was displayed in Fig. 4. From the representative Cho/NAA ratio maps, we can see the Cho/NAA ratios in the tumor

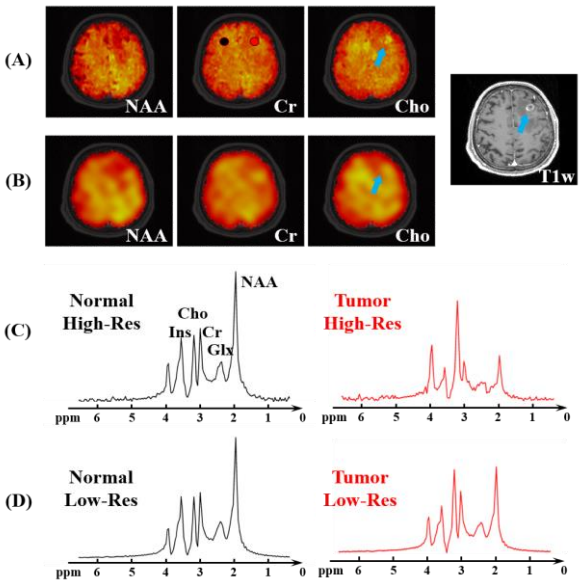

Figure 2. A representative set of MRSI results obtained from a brain tumor patient. (A) High-resolution metabolite maps using the proposed method (2.0×3.0×3.0 mm^3). (B) Low-resolution metabolite maps with a practically used resolution (12×12×12 mm^3). (C) Spectra from normal tissue (black dot) and tumor (red dot), respectively, which were obtained by the proposed high-resolution MRSI method. (D) Spectra from the same points as in (C) but obtained by the traditional low-resolution MRSI method.

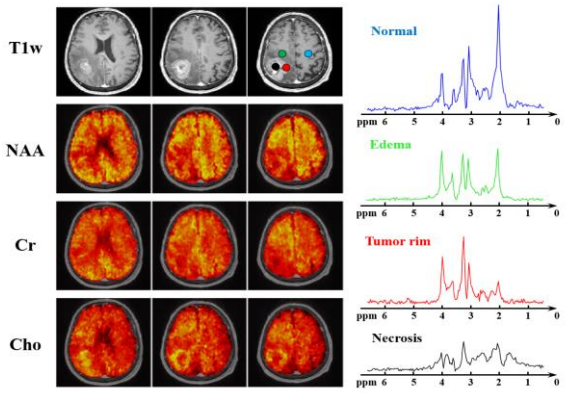

Figure 3. Representative MRSI results obtained from a patient with high-grade glioma. Localized spectra from the normal tissue, edema, enhancing ring, and necrosis core showed distinct spectral features. The high-resolution metabolite maps clearly showed the spatial intra-tumoral heterogeneity.

lesions were higher than the normal tissues, and the ratios in high-grade tumor were higher than the low-grade tumor, which is consistent with previous studies [3], [7]. Analyzing the Cho/NAA values between two groups quantitatively (three patients in each group, all voxels in the tumor and contralateral normal tissues were counted), we can see the significant differences of Cho/NAA values between high-grade tumor and low-grade tumor ($P<0.0001$) and between tumor and normal tissues ($P<0.0001$).

Our proposed imaging method was also applied to monitoring the longitudinal metabolic changes after treatment on a tumor (metastasis from lung cancer) patient. Three scans were performed on the patient in 2 weeks, 3 months, and 6 months after the gamma knife therapy, respectively. The Cho/NAA maps and quantitative values in the lesion area were

shown in Fig. 5. We can clearly see the reduction of Cho/NAA along the time, which is related to the regional remission and reduction of tumor volume (can be observed on the anatomical images). These longitudinal positive responses to the treatment were well-captured by the metabolic changes detected using the presented method.

These preliminary clinical results with a small cohort of patients demonstrated the feasibility and potential of our proposed method in capturing small brain tumors, imaging tumor heterogeneities, tumor characterization and monitoring treatment responses. This work could lay a foundation for further metabolic studies on brain tumors, providing more clinical insights.

IV. Conclusion

A new technique for high-resolution label-free molecular imaging has been developed for tumor imaging using MR spectroscopic signals. The technique enables 3D mapping of brain tumor metabolites at a nominal spatial resolution of $2.0\times3.0\times3.0$ mm^3 in a 7-minute scan. This new imaging capability has produced encouraging experimental results capturing metabolic alterations in small-size tumors and revealing tumor heterogeneities, which are clinically useful for tumor grading and monitoring treatment effects.

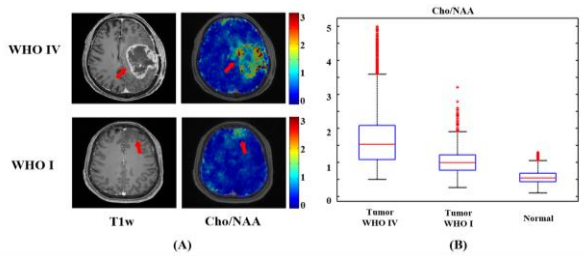

Figure 4. (A) Representative Cho/NAA maps from a high-grade tumor (WHO IV) and a low-grade tumor (WHO I). (B) Quantitative Cho/NAA values in the high-grade tumor (from 3 patients), low-grade tumor (from 3 patients), and corresponding contralateral normal tissues. The central red mark is the median, the edges of the box are the 25th and 75th percentiles.

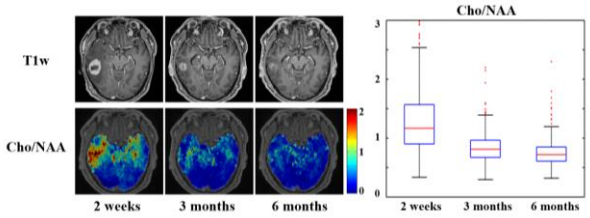

Figure 5. Longitudinal metabolic changes of a tumor patient in 2 weeks, 3 months, and 6 months after the gamma knife therapy. The recoveries of NAA and Cho along time have been observed from both spatial maps and quantitative values of Cho/NAA in the tumor regions.

References

[1] J. L. Spratlin, N. J. Serkova, and S. G. Eckhardt, "Clinical applications of metabolomics in oncology: A review," *Clinical Cancer Research*, vol. 15, no. 2. pp. 431–440, 2009.

[2] V. Kumar, U. Sharma, and N. R. Jagannathan, "In vivo magnetic resonance spectroscopy of cancer," *Biomed. Spectrosc. Imaging*, vol. 1, no. 1, pp. 89–100, 2012.

[3] G. Lin, K. R. Keshari, and J. M. Park, "Cancer metabolism and tumor heterogeneity: Imaging perspectives using MR imaging and spectroscopy," *Contrast Media and Molecular Imaging*, vol. 2017. 2017.

[4] G. Verma *et al.*, "Non-invasive detection of 2-hydroxyglutarate in IDH-mutated gliomas using two-dimensional localized correlation spectroscopy (2D L-COSY) at 7 Tesla," *J. Transl. Med.*, vol. 14, no. 1, 2016.

[5] M. J. Fulham *et al.*, "Mapping of brain tumor metabolites with proton MR spectroscopic imaging: Clinical relevance," *Radiology*, vol. 185, no. 3, pp. 675–686, 1992.

[6] M. C. Preul *et al.*, "Accurate, noninvasive diagnosis of human brain tumors by using proton magnetic resonance spectroscopy," *Nat. Med.*, vol. 2, no. 3, pp. 323–325, 1996.

[7] A. Horská and P. B. Barker, "Imaging of brain tumors: MR spectroscopy and metabolic imaging," *Neuroimaging Clinics of North America*, vol. 20, no. 3. pp. 293–310, 2010.

[8] G. Öz *et al.*, "Clinical proton MR spectroscopy in central nervous system disorders," *Radiology*, vol. 270, no. 3. pp. 658–679, 2014.

[9] W. Chen, "Clinical applications of PET in brain tumors," *Journal of Nuclear Medicine*, vol. 48, no. 9. pp. 1468–1481, 2007.

[10] K. Herholz, "Brain Tumors: An Update on Clinical PET Research in Gliomas," *Seminars in Nuclear Medicine*, vol. 47, no. 1. pp. 5–17, 2017.

[11] O. C. Andronesi, B. A. Gagoski, and A. G. Sorensen, "Neurologic 3D MR spectroscopic imaging with low-power adiabatic pulses and fast spiral acquisition," *Radiology*, 2012.

[12] A. Haase, J. Frahm, W. Hanicke, and D. Matthaei, "1H NMR chemical shift selective (CHESS) imaging," *Physics in Medicine and Biology*. 1985.

[13] M. Chiew *et al.*, "Density-weighted concentric rings k-space trajectory for 1H magnetic resonance spectroscopic imaging at 7 T," *NMR Biomed.*, 2018.

[14] S. Posse, G. Tedeschi, R. Risinger, R. Ogg, and D. Le Bihan, "High Speed 1H Spectroscopic Imaging in Human Brain by Echo Planar Spatial-Spectral Encoding," *Magn. Reson. Med.*, 1995.

[15] E. Adalsteinsson, P. Irarrazabal, S. Topp, C. Meyer, A. Macovski, and D. M. Spielman, "Volumetric spectroscopic imaging with spiral-based k-space trajectories," *Magn. Reson. Med.*, 1998.

[16] R. Eslami and M. Jacob, "A sparse reconstruction algorithm for parallel spiral MR spectroscopic imaging," in *Proceedings - International Symposium on Biomedical Imaging*, 2011.

[17] F. H. Lin *et al.*, "Sensitivity-encoded (SENSE) proton echo-planar spectroscopic imaging (PEPSI) in the human brain," *Magn. Reson. Med.*, 2007.

[18] J. Kornak, K. Young, B. J. Soher, and A. A. Maudsley, "Bayesian κ-Space time reconstruction of MR spectroscopic imaging for enhanced resolution," *IEEE Trans. Med. Imaging*, 2010.

[19] Z. P. Liang, "Spatiotemporal imaging with partially separable functions," in *2007 4th IEEE International Symposium on Biomedical Imaging: From Nano to Macro - Proceedings*, 2007, pp. 988–991.

[20] F. Lam and Z. P. Liang, "A subspace approach to high-resolution spectroscopic imaging," *Magn. Reson. Med.*, vol. 71, no. 4, pp. 1349–1357, 2014.

[21] F. Lam, C. Ma, B. Clifford, C. L. Johnson, and Z. P. Liang, "High-resolution 1H-MRSI of the brain using SPICE: Data acquisition and image reconstruction," *Magn. Reson. Med.*, vol. 76, no. 4, pp. 1059–1070, 2016.

[22] X. Peng, F. Lam, Y. Li, B. Clifford, and Z. P. Liang, "Simultaneous QSM and metabolic imaging of the brain using SPICE," *Magn. Reson. Med.*, vol. 79, no. 1, pp. 13–21, 2018.

[23] Y. Li, F. Lam, B. Clifford, and Z. P. Liang, "A subspace approach to spectral quantification for MR spectroscopic imaging," *IEEE Trans. Biomed. Eng.*, vol. 64, no. 10, pp. 2486–2489, 2017.

[24] Z.-P. L. F. Lam, B. Clifford, C. Ma, C. L. Johnson, "Ultra-high resolution 3D 1H-MRSI of the brain: Subspace-based data acquisitions and processing," in *Int. Soc. Magn. Reson. Med.*, 2015, p. 2370.

[25] R. Guo *et al.*, "Simultaneous QSM and metabolic imaging of the brain using SPICE: Further improvements in data acquisition and processing," *Magn. Reson. Med.*, vol. 85, no. 2, pp. 970–977, 2021.

[26] F. Lam, Y. Li, R. Guo, B. Clifford, and Z. P. Liang, "Ultrafast magnetic resonance spectroscopic imaging using SPICE with learned subspaces," *Magn. Reson. Med.*, vol. 83, no. 2, pp. 377–390, 2020.

[27] R. Guo, Y. Zhao, Y. Li, Y. Li, and Z. P. Liang, "Simultaneous metabolic and functional imaging of the brain using SPICE," *Magn. Reson. Med.*, vol. 82, no. 6, pp. 1993–2002, 2019.